Thermodynamics of the Adsolubilization Equilibrium of Rhodamine B by Surfactant-Modified Zeolites

Katumitu Hayakawa,* Yukihiko Miyamoto, Junichi Kurawaki, Yoshifumi Kusumoto, Iwao Satake, and Masashi Sakai†

Department of Chemistry and BioScience, Faculty of Science, Kagoshima University, 1-21-35 Korimoto, Kagoshima 890-0065

†Department of Industrial Chemistry, Faculty of Engineering, Kyushu Sangyou University, 2-3-1 Matsukadai, Higashi-ku, Fukuoka 813-8503

(Received January 31, 2000)

The adsolubilization of the cationic dye rhodamine B (RB) into the adsorbed layers of dodecyl- (DTAB) and tetradecyltrimethylammonium bromide (TTAB) on high silica mordenites (HSZ-1, HSZ-3) and P-type zeolite (PZ) was examined quantitatively. The adsolubilization constant for the HSZ-1/TTAB system was determined at temperatures from 10 to 40 °C. As the surfactant adsorption increased, the adsolubilization of RB by the zeolite/surfactant complexes was enhanced. Adsolubilization of RB by HSZ-3/surfactant complexes required a critical quantity of adsorbed surfactant, whereas the PZ/TTAB complex needed only a very small quantity of adsorbed TTAB to adsolubilize RB. Both the adsolubilization constant and the maximum capacity were calculated using a Langmuir-type equation, and the enthalpy and entropy changes were determined for the HSZ-1/TTAB mixed system. The difference in the adsolubilization mode of the three zeolite/surfactant complexes is discussed in relation to the aggregation mode of the cationic surfactant.

Zeolites with small pores are often useless for chemical reactions and as a molecular sieve of guest organic molecules due to inaccessibility of the pores. The adsorption of a surfactant on various solid surfaces is reported to induce or enhance the coadsorption of a second solute that is not adsorbed on the solid without the surfactant.[1—20] This phenomenon has been ascribed to the formation of surfactant aggregates on solid surfaces; the term adsolubilization or surface solubilization is defined as the solubilization of nonpolar molecules by adsorbed surfactant aggregates on a solid surface.[7,21,22] Probing studies using spectroscopy have revealed the formation of surfactant aggregates in hemimicelles or admicelles on various solid particles in aqueous suspensions.[22—34] These observations suggest that zeolite–surfactant complexes are capable of incorporating hydrophobic compounds, such as surfactant micelles, to solubilize water-insoluble compounds in the hydrophobic core. Indeed, some hydrophobic dyes that are not adsorbed at the interface between mineral particles and water can be coadsorbed in the presence of surfactants.[7,9,21,35,36]

We have observed the enhancement of the fluorescence intensity of pyrene on a zeolite surface in the presence of cationic surfactants,[33] indicating the coadsorption of pyrene and cationic surfactants at a zeolite/water interface. In this study, we quantified the coadsorption of rhodamine B (RB) by surfactant complexes of high silica mordenites (HSZ-1, HSZ-3) and P-type zeolite (PZ) and determined the adsolubilization constant for different quantities of the adsorbed surfactant. The adsolubilization constant of the HSZ-1/surfactant system was determined at different temperatures, and the thermodynamic parameters were estimated for the adsolubilization of RB.

Experimental

Materials. Two high-silica mordenites (abbreviated as HSZ-1 for HSZ-610NAA and HSZ-3 for HSZ-640NAA, Toso, Tokyo) and P-type zeolite (abbreviated as PZ, Sankei Chemicals, Kagoshima) were used. The respective pore diameters were 0.7 nm for both HSZ-1 and HSZ-3, and 0.4 nm for PZ; also the respective specific surface areas were 310, 340, and 65.3 $m^2 g^{-1}$, as indicated by the manufacturer. Porosimetry on PZ with a Shimadzu-micromeritex Assap 2400 surface-area porosimeter revealed mesopores of 7.5 nm. The respective Si/Al ratios were 5.40 for HSZ-1, 9.23 for HSZ-3, and 2.00 for PZ. Before use, the zeolites were extensively washed with doubly distilled water, dried under reduced pressure at 110 °C, and dried again for 2 h at 100 °C under reduced pressure. The surfactants used were tetradecyltrimethylammonium bromide (TTAB) and dodecyltrimethylammonium bromide (DTAB) (GR grade from TCI, Tokyo); they were purified by repeated recrystallization from acetone. Rhodamine B (GR grade from Wako, Osaka) was used as received.

Measurements. Mixtures of a fixed weight of zeolite and a fixed volume of surfactant stock solution were first equilibrated for surfactant adsorption for at least 48 h with stirring at a constant temperature. Various amounts of RB stock solution and water were added to the suspensions (the total volume of the solution was adjusted to 15 mL) and equilibrated for an additional 24 h. The solution pH varied between 9.2 and 9.7. Supernatant aliquots separated by centrifugation were withdrawn for potentiometry with a surfactant ion-selective electrode and spectrophotometry of unbound RB using a Hitachi Spectrophotometer (Type 228). Cali-

bration measurements confirmed a linear relationship between the absorbance at 555 nm and the concentration of aqueous RB solutions up to an absorbance of 1.5. The molar absorbance was estimated at 9.1×10^4 mol^{-1} dm^3 cm^{-1}. The calibration curve was convex downward above an absorbance of 1.5, due to the formation of the RB dimer.[37] Only the absorbance data below 1.5 were used for determining the concentration of unbound RB. Since the concentrations of the surfactant were below the critical micelle concentration (16 mmol dm^{-3} for DTAB and 3.6 mmol dm^{-3} for TTAB), solubilization in surfactant micelles was excluded. The quantity of the surfactant adsorbed on the zeolite was determined by potentiometry with a following surfactant ion-selective electrode.

Ag–AgCl electrode	Agar	Test solution	Functional membrane

Reference solution	Agar	Ag–AgCl electrode

The functional membrane consists of 25% poly(vinyl chloride) 74% bis(2-ethylhexyl) phthalate as plasticizer, and a 0.8% carrier complex. This electrode has proved to have good selectivity for DTAB and TTAB ions with a nearly Nernst response, even in the presence of excess inorganic ions.

Results and Discussion

The RB absorption spectra were measured in both the presence and absence of zeolites and surfactants. The absorbance of solutions without a surfactant was very close to that of an aqueous solution, but greatly decreased in the presence of a surfactant together with zeolite. The dependence of the absorbance of the supernatant at 555 nm in the presence of HSZ-3 on the total concentration of RB at various TTAB concentrations is given in Fig. 1. The plots almost coincide with the calibration curve (solid line) until 0.7 mmol dm^{-3} TTAB (a, b, c), indicating no incorporation of RB. Above that concentration, the plots deviate downward due to the incorporation of RB by the zeolite/surfactant complexes.

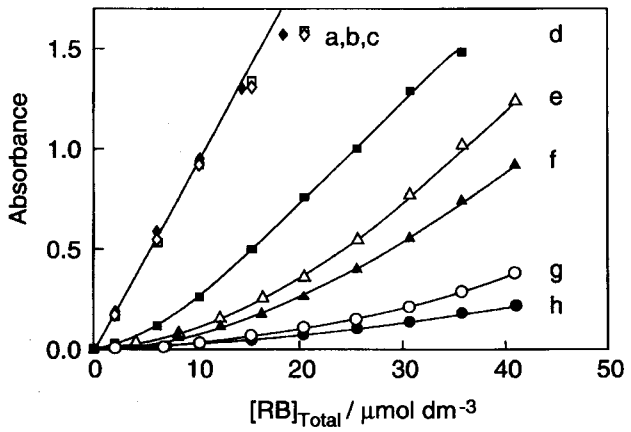

Fig. 1. Absorbance of RB in the supernatant of HSZ-3/TTAB mixed suspensions. The total concentration of TTAB: a. 0.0, b. 0.3, c. 0.7, d. 1.0, e. 1.2, f. 1.4, g. 1.7, h. 2.0 mmol dm^{-3}. The straight line indicates the calibration for the determination of unbound RB. The curves through the points are only guides to the eye.

The specific amount of incorporated RB (X_{RB}) was calculated from the absorbance decrease shown in Fig. 1, and was plotted against the concentration of added surfactant ([S]) for the HSZ-3/TTAB and HSZ-3/DTAB systems shown in Fig. 2. At low surfactant concentrations, the HSZ-3/surfactant complexes do not incorporate any RB. Above a critical surfactant concentration, a sharp increase is observed in the amount of incorporated RB. Since the surfactants were already adsorbed at concentrations below the critical concentration,[38] this observation suggests that RB is incorporated by the surfactant aggregates on the zeolite surface. Therefore, the incorporation of RB by HSZ-3/surfactant complexes is ascribed to the adsolubilization or surface solubilization.[21,22]

The adsolubilization isotherms are given in Figs. 3, 4, 5, and 6 for the HSZ-3/DTAB, HSZ-3/TTAB, and PZ/TTAB complexes at 25 °C, and for the HSZ-1/TTAB complex at 20 °C at various concentrations of added surfactant. Since the isotherms show Langmuir-type adsorption at higher concentrations of the surfactant, we analyzed the adsolubilization isotherms in Figs. 3, 4, 5, and 6 using the following equation:

$$X_{RB} = \frac{K[RB]_f}{1 + K[RB]_f} X_{max} \quad (1)$$

where K is the equilibrium constant for the adsolubilization reaction, X_{max} is the maximum capacity for the adsolubilization of RB by the zeolite/surfactant complexes, and $[RB]_f$ is the equilibrium concentration of RB in bulk solutions. This equation was derived from the following adsolubilization model:

$$\text{RB (in Bulk)} \overset{K}{\rightleftarrows} \text{RB (in Complex)} \quad (2)$$

Equation 1 was applied to plots of X_{RB} vs. $[RB]_f$, and the values of K and X_{max} that give the best fits to the experimental data were obtained by a curve-fitting method (Table 1). The solid curves in Figs. 3, 4, 5, and 6 were calculated using these values. Table 1 also includes the amount of surfactant adsorbed on 1.0 g zeolite, X_S.

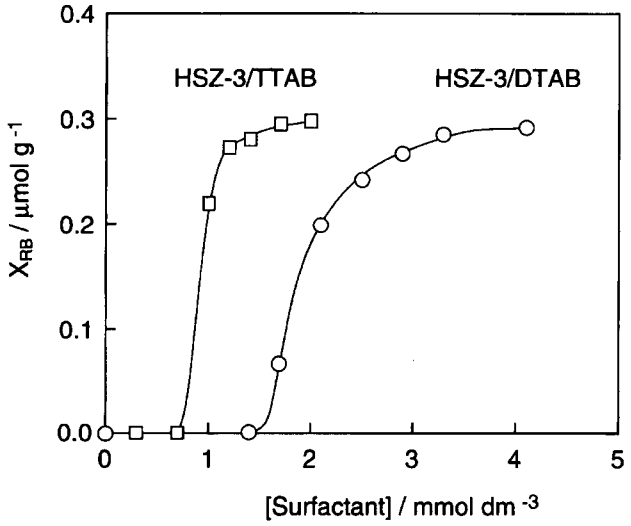

Fig. 2. Dependence of the amount of adsolubilized RB on the surfactant concentration. The curves through the points are only guides to the eye.

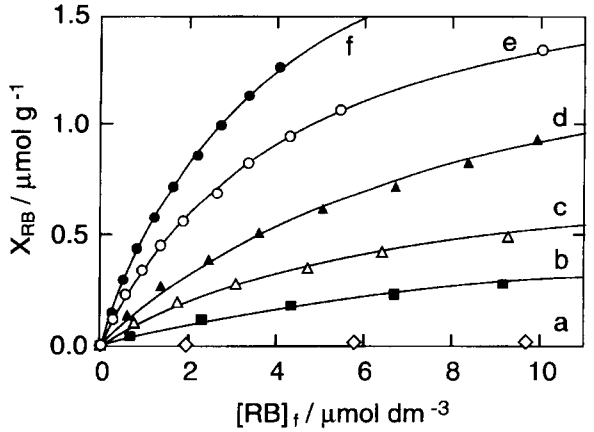

Fig. 3. Adsolubilization isotherms of RB by HSM-3/DTAB mixed system at 25 °C. The concentration of DTAB: a. 1.7, b. 2.1, c. 2.5, d. 2.9, e. 3.3, f. 4.1 mmol dm^{-3}. The curves are calculated by Eq. 1 using the values for K and X_{max} given in Table 1.

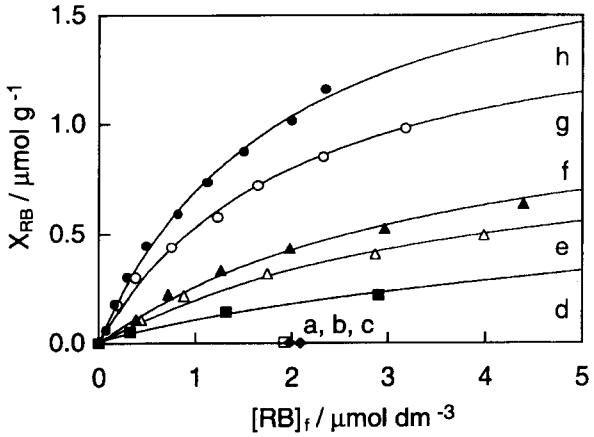

Fig. 4. Adsolubilization isotherms of RB by HSM-3/TTAB mixed system at 25 °C. The concentration of TTAB: a. 0.0, b. 0.3, c. 0.7, d. 1.0, e. 1.2, f. 1.4, g. 1.7, h. 2.0 mmol dm^{-3}. The curves are calculated by Eq. 1 using the values for K and X_{max} given in Table 1.

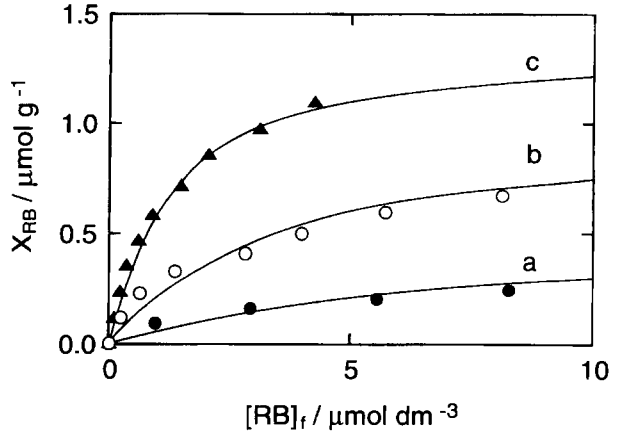

Fig. 5. Adsolubilization isotherms of RB by PZ/TTAB mixed system at 25 °C. The concentration of TTAB: a. 0.08, b. 0.20, c. 0.50 mmol dm^{-3}. The curves are calculated by Eq. 1 using the values for K and X_{max} given in Table 1.

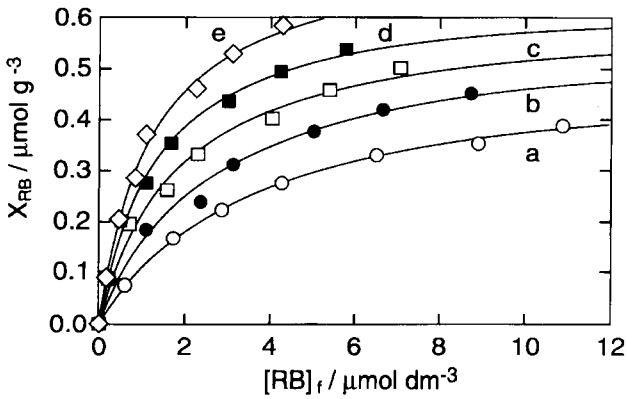

Fig. 6. Adsolubilization isotherms of RB by HSM-1/TTAB mixed system at 20 °C. The concentration of TTAB: a. 0.10, b. 0.125, c. 0.15, d. 0.175, e. 0.20 mmol dm^{-3}. The curves are calculated by Eq. 1 using the values for K and X_{max} given in Table 1.

Table 1 clearly indicates that both the adsolubilization constant and the maximum adsolubilization capacity increase as the quantity of bound surfactant increases (Fig. 7). The adsorption density values of the surfactants, Γ_S, calculated by the ratio of X_S to the specific surface area of zeolite, were 0.36×10^{-6} mol m^{-2} for HSZ-3/DTAB, 0.18×10^{-6} mol m^{-2} for HSZ-3/TTAB, 0.23×10^{-6} mol m^{-2} for PZ/TTAB, and 0.019×10^{-6} mol m^{-2} for HSZ-1/TTAB at the highest concentrations of surfactant. From these values, the average area occupied by a surfactant ion was calculated to be 460 nm^2 for the HSZ-3/DTAB system, 920 nm^2 for the HSZ-3/TTAB system, and 720 nm^2 for the PZ/TTAB system. These areas are much larger than the area occupied by a laterally oriented surfactant layer at the water–air interface. It is impossible for the surfactant to form aggregates on the zeolite surface at this low adsorption density. This unlikely result is caused by the use of the total surface area in this estimation. We conclude that only the outer surface of the zeolite is effective for surfactant adsorption, because of its small pores and the fact that surfactant aggregation occurs on the outer surface.

A rough estimation of the slope of X_{max} versus X_S plots gives 0.031, 0.044, 0.060, and 0.09 for the HSZ-3/DTAB, HSZ-3/TTAB, PZ/TTAB, and HSZ-1/TTAB systems, respectively. These values suggest that, on average, the respective number of surfactant ions required for the adsolubilization of one RB molecule is 32, 23, 17, and 11 for the four complexes. Because each Al atom carries an anionic site in the zeolite frame, the Al/Si ratio is a measure of the hydrophilic property of zeolite. In other words, the Si/Al mole ratio is a measure of the hydrophobic property of zeolite. Since HSZ-3 (Si/Al = 9.23) is more hydrophobic than PZ (Si/Al = 2.00) and HSZ-1 (Si/Al = 5.40), the surfactant ion is strongly adsorbed through a hydrophobic interaction as well as electrostatic attraction.[38] The hydrophobic interaction between the zeolite surface and the surfactant ions interferes with surfactant aggregation where the hydrophobic interaction works among bound surfactant ions and induces a thin

Table 1. Thermodynamic Parameters for the Adsolubilization Equilibrium of RB by Some Zeolite–Cationic Surfactant Complexes

Adsorbed surfactant X_S/μmol g^{-1}	Maximum capacity X_{max}/μmol g^{-1}	Adsolubilization constant $K/10^6$	Gibbs energy change $\Delta G°$/kJ mol^{-1}	Temperature t/°C
	HSZ-3 / DTAB			
63	0.72	0.073	−37.7	
75	0.91	0.14	−39.3	
87	1.74	0.18	−39.9	25
99	1.94	0.22	−40.4	
123	2.48	0.25	−40.7	
(±5%)	(±0.06)	(±0.01)	(±0.2)	
	HSZ-3 / TTAB			
30	0.7	0.072	−37.7	
36	1.02	0.24	−40.6	
42	1.22	0.27	−40.9	25
51	1.62	0.49	−42.4	
60	2.04	0.52	−42.6	
(±5%)	(±0.09)	(±0.03)	(±0.4)	
	PZ / TTAB			
2.4	0.55	0.12	−38.9	
6	1.02	0.28	−41.0	25
15	1.37	0.84	−43.7	
(±5%)	(±0.08)	(±0.06)	(±0.7)	
	HSZ-1 / TTAB			
3	0.480	0.27	−40.3	
3.75	0.565	0.38	−41.1	
4.5	0.626	0.53	−41.9	20
5.25	0.698	0.63	−42.3	
6	0.749	0.92	−43.2	

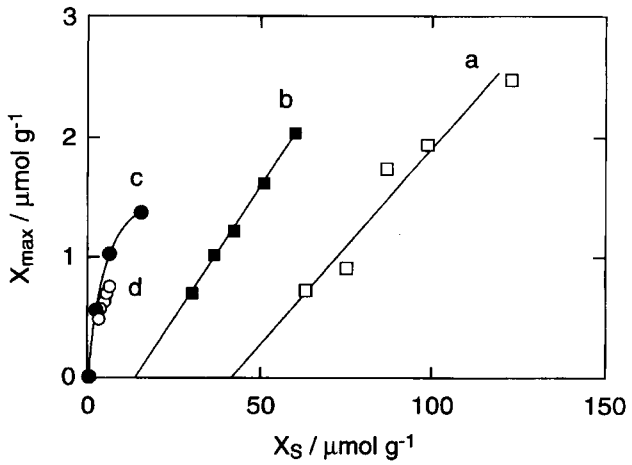

Fig. 7. Dependence of the maximum adsolubilized amount of RB on the bound surfactant quantities : a. HSZ-3/DTAB, b. HSZ- 3/TTAB, c. PZ/TTAB, d. HSZ- 1/TTAB. The curves through the points are only guides to the eye.

layer of adsorbed surfactant ions. Hence, this thin layer of surfactant aggregates on HSZ-3 may have a less solubilizing capacity. However, the X_{max} versus X_S plots in Fig. 7 indicate that a clear critical quantity of adsorbed surfactant was required for the adsolubilization of RB into HSZ-3/surfactant complexes. From this observation, we infer that no surfactant aggregates are present on the HSZ-3 surface before this critical quantity of bound surfactant is reached. On the other hand, the PZ/TTAB and HSZ-1/TTAB complexes incorporate RB when very little TTAB is adsorbed, suggesting the formation of surfactant aggregates on PZ and HSZ-1, even at a very low adsorption density of surfactant. The fluorescence spectrum of pyrene proved that a hydrophobic domain formed on PZ/TTAB complexes even at a very low adsorption density of the surfactant.[33] The increasing rate of the X_{max} versus X_S plots after the critical X_S for HSZ-3/surfactant complexes is smaller for the HSZ-3/DTAB system than for the HSZ-3/TTAB system. This observation suggests that once the surfactant aggregates on HSZ-3 grow large enough to adsolubilize RB, the adsolubilization capacity for RB is larger for TTAB, with its longer hydrophobic chain, than for DTAB.

The Gibbs-energy change for the adsolubilization of RB by the zeolite/surfactant complexes was calculated from K using the mole-fraction unit as the bulk concentration,

$$\Delta G° = -RT\ln(55.5\ K) \quad (3)$$

The values are listed in Table 1. Figure 8 shows the dependence of the Gibbs energy change on X_S. The fact that $\Delta G°$ decreases with X_S suggests that there is not sufficient amount of surfactant aggregate to form a pseudophase on the

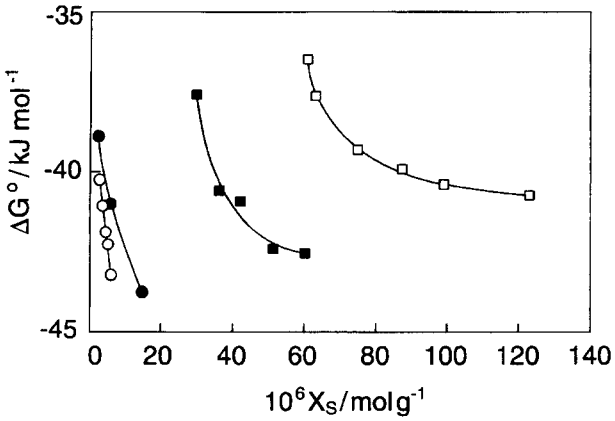

Fig. 8. Dependence of Gibbs function of adsolubilization of RB by the zeolite/surfactant mixed systems: a. HSZ-3/DTAB, b. HSZ-3/TTAB, c. PZ/TTAB, d. HSZ-1/TTAB. The curves through the points are only guides to the eye.

Table 2. Temperature Dependence of the Adsolubilization Constant of RB by HSZ-1/TTAB Complexes and the Thermodynamic Parameters at 20 °C

Temperature T/K	Adsolubilization constant, $10^{-6}K$ (mol^{-1} dm^3)				
283	0.31	0.49	0.66	0.87	1.46
293	0.27	0.38	0.54	0.63	0.92
303	0.21	0.32	0.36	0.45	0.56
313	0.19	0.25	0.30	0.34	0.36
X_S/μmol g^{-1}	3.00	3.75	4.50	5.25	6.00
$\Delta H°$/kJ mol^{-1}	−13.0	−16.5	−20.3	−23.0	−34.6
$\Delta G°$/kJ mol^{-1}	−40.3	−41.1	−41.9	−42.3	−43.2
$\Delta S°$/J K^{-1} mol^{-1}	93	84	74	66	29

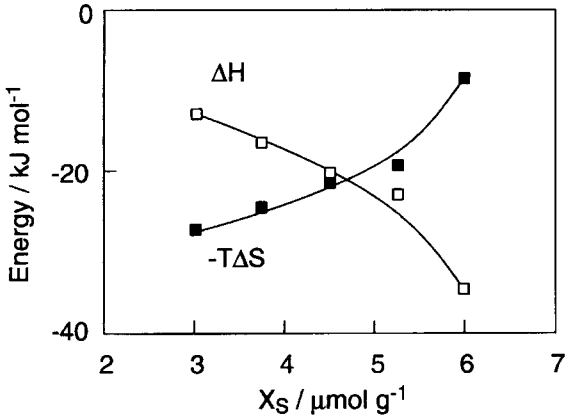

Fig. 9. Comparison of entropic and enthalpic contributions for the adsolubilization of RB by HSZ-1/TTAB complexes.

zeolite for partitioning RB between the aqueous phase and the adsorbed surfactant aggregates.

The higher Gibbs-energy change, that is, the lower adsolubilization constant for the HSZ-3/DTAB complex than for HSZ-3/TTAB, even at a higher surfactant adsorption density, indicates the lower adsolubilization power of DTAB, with its short chain, as is often observed in the micellar solubilization of surfactants.[39]

The surfactant aggregation on a solid surface is induced by a cooperative interaction among the bound surfactants. At a low adsorption density, TTAB does not form any aggregates on HSZ-3 because of the strong hydrophobic interaction between TTAB and HSZ-3. This leads to no adsolubilization of RB. On the other hand, TTAB on PZ or HSZ-1 does form aggregates, because of the hydrophobic interaction between the bound surfactants at a low adsorption density of the surfactant, and adsolubilizes RB in spite of the weak surfactant adsorption.[33,38] A similar solubilization property has been observed for a water-insoluble dye (*o*-(2-amino-1-naphthylazo)toluene) in polyelectrolyte/surfactant complexes.[40] Although poly(styrenesulfonate) (PSS) binds DTAB much more strongly than does dextran sulfate (DxS), the dye is less solubilized by the PSS/DTAB complex than by the DxS/DTAB complex. PSS is more hydrophobic than DxS. In the present systems, TTAB may aggregate more readily on PZ or HSZ-1 than on HSZ-3 due to the hydrophobic interaction among the surfactant chains adsorbed on PZ or HSZ-1. The Gibbs-energy change for the HSZ-3/TTAB complex tends to converge to -43 kJ mol^{-1} at an adsorption density of about 60×10^{-6} mol g^{-1}, suggesting that the aggregates grow large enough to solubilize RB.

Although the HSZ-1/TTAB complex shows a similar Gibbs energy change at a lower surfactant adsorption density than the PZ/TTAB complex (Fig. 8), the adsolubilization capacity is lower for the HSZ-1/TTAB complex than for the PZ/TTAB complex (Fig. 7). Because the adsolubilization affinity is not different, both complexes may have similar surfactant aggregates on the outer surface. Supposing that the Gibbs-energy change depends on the aggregate size of surfactant adsorbed on the outer surface of the zeolite, we infer that a large size, but a small number of aggregates, is formed on the outer surface of the HSZ-1/TTAB complex from Figs. 7 and 8. The large aggregates at the low adsorption density of TTAB may be induced from the small outer surface of HSZ-1.

The adsolubilization constant was determined at different temperatures for the HSZ-1/TTAB system; the values are given in Table 2. The constant decreases as the temperature increases, indicating that adsolubilization is an exothermic process. The enthalpy and entropy changes were calculated from the temperature dependence, and are listed in Table 2. Both a decrease in enthalpy and a gain in entropy enhance the adsolubilization of RB, but the entropic contribution dominates at a low adsorption density of the surfactant, while the enthalpic contribution becomes dominant at a high adsorption density of the surfactant, as shown in Fig. 9. This suggests that the bulky surfactant aggregates at a low surfactant adsorption become more compact, leading to a strong hydrophobic attraction and constraining RB.

Conclusion

Although RB was adsolubilized by both PZ/TTAB and HSZ-3/cationic surfactant complexes, for the HSZ-3 system this only occurred above a critical concentration of the

surfactant. The adsolubilization constant and the Gibbs energy change were determined. Although the interaction of surfactant is stronger for hydrophobic HSZ-3 than for PZ, weak adsolubilization was observed for HSZ-3/surfactant complexes. This was ascribed to the weak aggregation of the surfactant on HSZ-3 due to the strong hydrophobic interaction between them.

This work was supported by a Grant-in-Aid for Scientific Research No. 09640693 from the Ministry of Education, Science, Sports and Culture, and in part by The Kagoshima Science Scholarship Foundation.

References

1 K. Esumi, M. Shibayama, and K. Meguro, *Langmuir*, **6**, 826 (1990).

2 E. Klumpp, H. Heitmann, and M. J. Schwuger, *Colloids Surf. A*, **78**, 93 (1993).

3 V. Monticone, M. H. Mannebach, and C. Treiner, *Langmuir*, **10**, 2395 (1994).

4 V. Monticone and C. Treiner, *Langmuir*, **11**, 1753 (1995).

5 K. Esumi, K. Mizuno, and Y. Yamanaka, *Langmuir*, **11**, 1571 (1995).

6 G. P. Funkhouser, M. P. Arévalo, D. T. Glatzhofer, and E. A. O'Rear, *Langmuir*, **11**, 1443 (1995).

7 D. Stigter, R. J. Williams, and K. J. Mysels, *J. Phys. Chem.*, **59**, 330 (1955).

8 V. Monticone and C. Treiner, *J. Colloid Interface Sci.*, **166**, 394 (1994).

9 B.-Y. Zhu, X. Zhao, and T. Gu, *J. Chem. Soc., Faraday Trans. 1*, **84**, 3951 (1988).

10 J. Jansen, C. Treiner, C. Vaution, and P. Puisieux, *Int. J. Pharm.*, **103**, 19 (1994).

11 V. Monticone and C. Treiner, *Colloids Surf. A*, **104**, 285 (1995).

12 K. Esumi, M. Matoba, and Y. Yamanaka, *Langmuir*, **12**, 2130 (1996).

13 T. R. Desai and S. G. Dixit, *J. Colloid Interface Sci.*, **179**, 544 (1996).

14 B. Kitiyanan, J. H. O'Haver, J. H. Harwell, and S. Osuwan, *Langmuir*, **12**, 2162 (1996).

15 R. N. Ward, P. B. Davies, and C. D. Bain, *J. Phys. Chem. B*, **101**, 1594 (1997).

16 K. Esumi, S. Uda, M. Goino, K. Ishizuki, T. Suhara, H. Fukui, and Y. Koide, *Langmuir*, **13**, 2803 (1997).

17 K. Esumi, Y. Takeda, M. Goino, K. Ishizuki, and Y. Koide, *Langmuir*, **13**, 2585 (1997).

18 K. Esumi, H. Toyoda, M. Goino, T. Suhara, and H. Fukui, *Langmuir*, **14**, 199 (1998).

19 K. Esumi, S. Uda, T. Suhara, H. Fukui, and Y. Koide, *J. Colloid Interface Sci.*, **193**, 315 (1997).

20 P. Favoriti and C. Treiner, *Langmuir*, **14**, 7493 (1998).

21 C. C. Nunn, R. S. Schechter, and W. H. Wade, *J. Phys. Chem.*, **86**, 3271 (1982).

22 J. H. Harwell, J. C. Hoskins, R. S. Schechter, and W. H. Wade, *Langmuir*, **1**, 251 (1985).

23 D. W. Fuerstenau, *J. Phys. Chem.*, **60**, 981 (1956).

24 P. Somasundaran and D. W. Fuerstenau, *J. Phys. Chem.*, **70**, 90 (1966).

25 K. C. Waterman, N. J. Turro, P. Chandar, and P. Somasundaran, *J. Phys. Chem.*, **90**, 6828 (1986).

26 P. Chandar, P. Somasundaran, K. C. Waterman, and N. J. Turro, *J. Phys. Chem.*, **91**, 148 (1987).

27 M. A. Yeskie and J. H. Harwell, *J. Phys. Chem.*, **92**, 2346 (1988).

28 P. Somasundaran, J. T. Kunjappu, C. V. Kumar, N. J. Turro, and J. K. Barton, *Langmuir*, **5**, 215 (1989).

29 J. H. Harwell and M. A. Yeskie, *J. Phys. Chem.*, **93**, 3372 (1989).

30 A. R. Rennie, E. M. Lee, E. A. Simister, and J. K. Thomas, *Langmuir*, **6**, 1031 (1990).

31 J. T. Kunjappu, P. Somasundaran, and N. J. Turro, *J. Phys. Chem.*, **94**, 8464 (1990).

32 T. Gu and H. Rupprecht, *Colloid Polym. Sci.*, **268**, 1148 (1990).

33 K. Hayakawa, M. Miyauchi, K. Uno, and I. Satake, *J. Surf. Sci. Technol.*, **8**, 217 (1992).

34 S. Manne, J. P. Cleveland, H. E. Gaub, G. D. Stucky, and P. K. Hansma, *Langmuir*, **10**, 4409 (1994).

35 K. Esumi, A. Sugimura, T. Yamada, and K. Meguro, *Colloids Surf.*, **62**, 249 (1992).

36 P. Mukerjee, R. Sharma, R. A. Pyter, and M. J. Gumkowski, "Surfactant Adsorption and Surface Solubilization," American Chemical Society, Washington, DC (1995), p. 22.

37 R. W. Chambers, T. Kajiwara, and D. R. Kearns, *J. Phys. Chem.*, **78**, 380 (1974).

38 K. Hayakawa, T. Morita, M. Ariyoshi, T. Maeda, and I. Satake, *J. Colloid Interface Sci.*, **177**, 621 (1996)

39 Y. Moroi and R. Matuura, *J. Colloid Interface Sci.*, **125**, 456 (1988).

40 K. Hayakawa, S. Shinohara, S. Sasawaki, I. Satake, and J. C. T. Kwak, *Bull. Chem. Soc. Jpn.*, **68**, 2179 (1995).